

Mechanical regulation of cardiac muscle by coupling calcium kinetics with cross-bridge cycling: a dynamic model

A. LANDESBERG AND S. SIDEMAN

Heart System Research Center, The Julius Silver Institute, and Department of Biomedical Engineering, Technion-Israel Institute of Technology, Haifa 32000, Israel

Landesberg, A., and S. Sideman. Mechanical regulation of cardiac muscle by coupling calcium kinetics with cross-bridge cycling: a dynamic model. *Am. J. Physiol.* 267 (*Heart Circ. Physiol.* 36): H779–H795, 1994.—This study describes the regulation of mechanical activity in the intact cardiac muscle, the effects of the free calcium transients and the mechanical constraints, and emphasizes the central role of the troponin complex in regulating muscle activity. A “loose coupling” between calcium binding to troponin and cross-bridge cycling is stipulated, allowing the existence of cross bridges in the strong conformation without having bound calcium on the neighboring troponin. The model includes two feedback mechanisms: 1) a positive feedback, or cooperativity, in which the cycling cross bridges affect the affinity of troponin for calcium, and 2) a negative mechanical feedback, where the filament-sliding velocity affects cross-bridge cycling. The model simulates the reported experimental force-length and force-velocity relationships at different levels of activation. The dependence of the shortening velocity on calcium concentration, sarcomere length, internal load, and rate of cross-bridge cycling is described analytically in agreement with reported data. Furthermore the model provides an analytic solution for Hill’s equation of the force-velocity relationship and for the phenomena of unloaded shortening velocity and force deficit. The model-calculated changes in free calcium in various mechanical conditions are in good agreement with the available experimental results.

excitation-contraction coupling; chemomechanical coupling; unloaded shortening velocity

CALCIUM IONS PLAY a central role in the regulation of excitation-contraction coupling. Measurements of the free calcium reveal different calcium transients with different contraction regimens and at different sarcomere lengths (2, 3); the decay of calcium transients in isotonic contractions is slow compared with the decay of the free calcium in isometric contractions (27), and an extra free calcium transient is evident after fast changes (quick release) of the sarcomere length (27). These data demonstrate the influence of the cycling cross bridges and length perturbations on the affinity of the regulatory proteins for calcium. The present model attempts to describe the intracellular control of contraction by coupling calcium binding to troponin with cross-bridge cycling and force development.

Models of cardiac muscle mechanics are usually based on the two fundamental mechanical characteristics: force-length (FLR) and force-velocity relationships (FVR) (5, 25, 35). However, these relationships are not unique characteristics of the contractile elements but depend on the activation level (17) and the prevailing mechanical conditions. Clearly, the ability to simulate cardiac muscle dynamics depends on a reasonable description of the

activation function and the complex relationship between calcium kinetics and cross-bridge cycling.

A major obstacle in modeling the excitation-contraction phenomena in the cardiac muscle is the ambiguity of the present definitions and descriptions of the mechanical activation function. Various activation functions have been used. Beyar and Sideman (5), for example, used a simple half-sinus mechanical activation function, and Wong (39) used an exponential activation function. Obviously, these deterministic functions cannot characterize the control of the excitation-contraction coupling. Izakov et al. (25) proposed a mechanical activation function that attempts to include the influence of the length, velocity, and two types of cooperativity mechanisms. Ford (17) summarized the debate on this issue and proposed to define the activation level by the number of sites on the thin filaments that are available for the attachment of myosin heads. Although the definition suggested by Ford cannot be experimentally quantified, it elucidates the activation mechanism and highlights the central role of the troponin-tropomyosin regulatory complexes (until now denoted simply as “troponin”) in coupling calcium kinetics with cross-bridge cycling and force development.

Three closely related concepts, or stipulations, guide the present attempt to characterize the control of the mechanical activity and the chemomechanical coupling.

1) The mechanical activation level is defined by coupling calcium binding to troponin with the regulation of cross-bridge cycling. Consistent with Ford’s definition of activation (17), the present model emphasizes the central role of troponin in regulating the excitation-contraction coupling. The activation level is considered to be the ability of the muscle to generate force, which is described by the number of available cross bridges in the weak non-force-generating conformation that can convert to the strong force-generating conformation. As shown below, this definition corresponds to the number of troponin units with bound calcium that are not associated with cross bridges at the strong conformation.

2) The mechanical performance of the muscle depends on its history. Thus, at a given time, length, load, and velocity, the muscle can demonstrate a different performance, depending on the path that the muscle has passed up to that point. This “memory” is expressed in the model by the state variables. As shown below, these states have a physiological meaning, e.g., the amount of calcium bound to troponin and the number of cross bridges at the strong conformation.

3) The chemomechanical coupling includes two feedback processes: a positive and a negative process (Fig. 1). The positive feedback, usually denoted as “cooperativ-

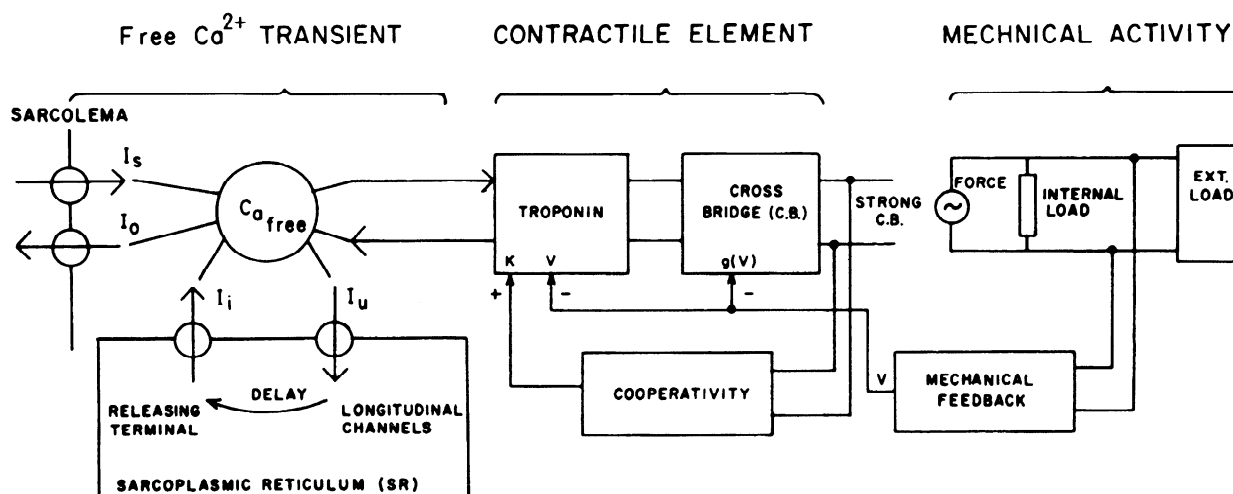


Fig. 1. Physiological model describes performances of contractile element and couples free calcium kinetics with mechanical activity. Model contains 2 main feedback mechanisms: a mechanical feedback and a positive feedback, termed cooperativity. I_i and I_s , calcium influx; I_o and I_u , calcium efflux; K , calcium-binding coefficient; V , sarcomere sliding velocity; $g(V)$, cross-bridge turnover from strong to weak conformation.

ity," is essentially biochemical; the conformations of the cross bridges affect the affinity of troponin for calcium. In the negative mechanical feedback loop, the shortening velocity of the filaments affects cross-bridge cycling rate. As shown below, these feedback mechanisms affect the FLR and FVR and alter the free calcium transients in various mechanical regimens.

The cooperativity mechanism is based here on our previous analysis (28) of experimental studies (21, 24, 26) with skinned cells at steady state, i.e., when the concentration of the free calcium is constant. The steady-state model is extended here to simulate the behavior of the intact cell, where the free calcium concentration is never at a steady state and the muscle is not solely subjected to isometric conditions. A dynamic model is used here to study the mechanical performance of the intact muscle in various mechanical loading conditions. The force and the free calcium have been analyzed and are compared with available experimental data obtained with intact cells.

Whereas the previous study established the basis for the cooperativity mechanism and the FLRs, the present study concentrates on the mechanical feedback and the FVRs.

PHYSIOLOGICAL MODEL

The analysis is based on the structural and biochemical model of cross-bridge cycling of Eisenberg, Hill, and Greene (16, 19). Their model suggests that the cross-bridge cycle is a repeated oarlike cycle between weak and strong conformations that differ in their structure and in their ability to generate force. The cross bridges cycle between the weak and the strong conformation because of nucleotide binding and release (16). ATP binding to myosin induces a structural change in the cross bridge; it weakens the binding of myosin to actin and transmits the myosin from the strong to the weak conformation. ATP hydrolysis and the release of phosphate causes the transition to the strong conformation.

Basic assumptions. The following assumptions are used to formulate the present model.

1) The regulatory unit consists of a single regulatory troponin complex with the adjacent seven actin molecules and the myosin heads.

2) The cross bridges exist essentially in a strong or a weak conformation. Force is produced only in the strong conformation (16).

3) The free head of the myosin and the actin-bound myosin are at rapid equilibrium. The cross bridges in the weak conformation jump easily from one actin site to another (16). Moreover, the cross bridges in the strong conformation can also attach and detach rapidly during force generation (8, 31).

4) The cross-bridge transitions between the weak and the strong conformations are described by the rate-limiting steps in the biochemical model of cross-bridge cycling (16). The rate-limiting step in the transition from the weak to the strong conformation is related to the hydrolysis of ATP and phosphate release (10).

5) The cross-bridge cycles between the weak and the strong conformations are independent of one another.

6) Each troponin molecule has three sites for binding calcium: two have high affinities and one has a low affinity for calcium (33). Calcium binding to either of the high-affinity sites is independent of calcium association with other binding sites in the whole sarcomere and has no effect on the regulation of cross-bridge cycling.

7) Calcium binding to the low-affinity sites regulates cross-bridge cycling. The major role of bound calcium is regulation of adenosinetriphosphatase (ATPase) activity (12), which is required for the transition of the cross bridges from the weak to the strong conformation. The activity of the ATPase is inhibited in the absence of calcium (12). Only an insignificant transition of cross bridges from the weak to the strong conformation occurs without calcium binding to the neighboring troponin site.

8) Troponin-tropomyosin-actin interactions along the sarcomere affect the kinetics of calcium binding to the low-affinity sites on the troponin along the sarcomere (18, 20).

9) Calcium can dissociate from the troponin before the transition of the cross bridges from the strong to the weak conformation; cross bridges can exist in the strong conformation without having bound calcium on the troponin. There is a loose coupling between cross-bridge weakening and calcium dissociation from the troponin, hence the term "loose-coupling" model.

10) There are three overlap regions between the thin (actin) and the thick (myosin) filaments (Fig. 2, top) along the sarcomere: a nonoverlap region, a single-overlap region, and a double-overlap region.

11) Cross-bridge cycling is not affected by the double-overlap of the actin filaments with the myosin filament; this is substantiated by measurement of the stiffness and the activity of the ATPase (36). However, the net force generated in the double-overlap region is zero (36). Consequently, the net force generated by the sarcomere is a function of the number of cross bridges in the strong conformation in the single-overlap region.

12) The heads of the myosin and the troponin complexes are distributed uniformly along the thick and thin filaments. The number of myosin heads in the single-overlap region depends linearly on the length of the single-overlap region, but the fraction of cross bridges in the strong conformation depends on calcium kinetics and cross-bridge cycling.

13) Filament-sliding velocity affects the rate of cross-bridge turnover from the strong to the weak conformation. The rate of transition from the strong to the weak conformation is affected by cross-bridge strain and thus by the filament-sliding velocity (16). To reduce energy losses, the ADP release from the strong cross bridges is slow, so the cross bridges will remain at the strong conformation until the work is completed (16). Consequently, the velocity of shortening has a direct effect on the rate of transition from the strong to the weak

conformation. A linear dependence of this cross-bridge weakening rate on the velocity of filament sliding is assumed here ($g = g_0 + g_1V$). This linear dependence is substantiated by Hill's equation (22) for the force-velocity relationship and by measurements of the force deficit by Leach et al. (29).

14) Filament sliding transfers troponin regulatory units at the edge of each region between the different overlap regions: from the nonoverlap to the single-overlap region and from the single-overlap to the double-overlap region as the muscle contracts; transfer occurs in the opposite direction as the muscle elongates during relaxation. The amount of troponin in each state that is transferred between these regions as a consequence of filament sliding is proportional to the sliding velocity of the filaments and the instantaneous density of the troponin in each state. The transfer of a state variable from the nonoverlap to the single-overlap region during muscle contraction depends on the amount of calcium bound to the thin filament in the nonoverlap region and on the number of cross bridges in the strong conformation on the thick filament in the single-overlap region.

15) The individual cross bridges act like Newtonian viscoelastic elements: the average FVRs of a single cross bridge are approximately linear. This assumption is based on the study of de Tombe and ter Keurs (14), who simultaneously measured the sarcomere force, the velocity of shortening, and the dynamic stiffness.

16) The internal load has a viscoelastic property, as measured by quick changes of muscle length at rest (14).

State variables of regulatory troponin complex. The population of the troponin regulatory proteins is divided into 10 groups or "states," as summarized in Table 1. These states are defined according to the following criteria: 1) the calcium is bound or unbound to the low-affinity sites of the troponin, 2) the cross bridges are in the strong or the weak conformation, and 3) the troponin is in the nonoverlap, single-overlap, or double-overlap region.

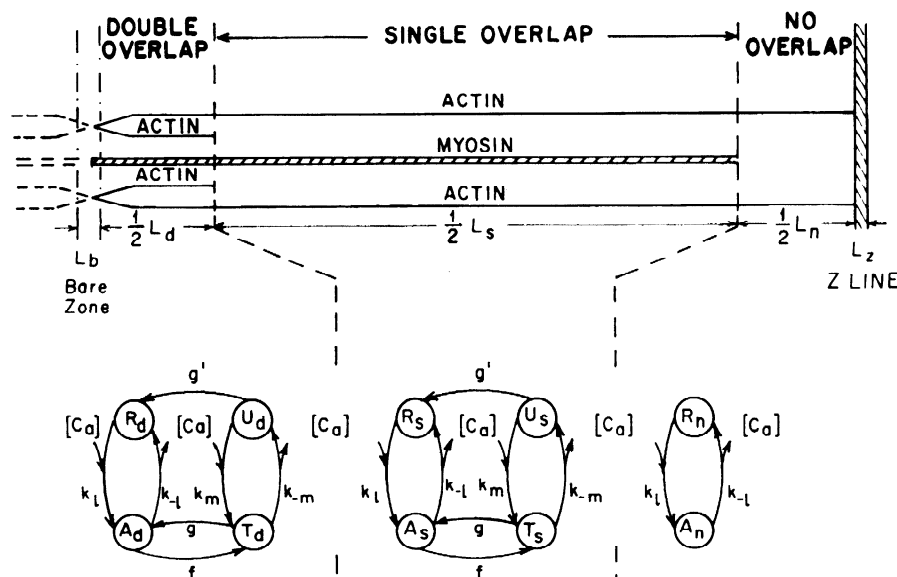


Fig. 2. Transitions between various states of troponin regulatory units in isometric regimen. Top: 3 distinct overlap regions in (half) sarcomere drawn for an overlap ratio $\alpha = 0.81$, sarcomere length = 1.9 μm , $L_s = 1.3 \mu\text{m}$, nonoverlap length (L_n) = double-overlap length (L_d) = 0.3 μm . Bottom: transitions between states are defined by calcium kinetics (k_1, k_{-1}, k_m, k_{-m}) and by cross-bridge cycling rates (f, g, g'). $[\text{Ca}]$, free calcium concentration.

Table 1. *State variables used in the model*

State of Troponin Complex	Overlap	Calcium	Cross Bridge
R _n	Non	Unbound	
A _n	Non	Bound	
R _s	Single	Unbound	Weak
A _s	Single	Bound	Weak
T _s	Single	Bound	Strong
U _s	Single	Unbound	Strong
R _d	Double	Unbound	Weak
A _d	Double	Bound	Weak
T _d	Double	Bound	Strong
U _d	Double	Unbound	Strong

R, resting state; A, activation, state that determines activation level; T, tension, state that determines amount of regulatory units that generate force and are associated with bound calcium; U, unbound, same as state T, but without bound calcium. Subscripts: n, nonoverlap; s, single overlap; d, double overlap.

Four states exist in the single-overlap region (R_s, A_s, T_s, and U_s), four in the double-overlap region (R_d, A_d, T_d, and U_d), and two in the nonoverlap region (R_n and A_n). The interactions between the troponin regulatory units are described in Fig. 2 for the isometric regimen. The transitions between the states are determined by the kinetics of calcium binding to troponin, the cross-bridge cycling, and the sliding velocity of the filaments.

The four states in the single-overlap region include R_s, which represents the rest state, wherein the cross bridges are in the weak conformation and no calcium is bound to the troponin. In A_s, calcium is bound to troponin but the cross bridges are still in the weak conformation. Cross-bridge cycling leads to T_s, where calcium is bound to the low-affinity sites and the cross bridges are in the strong force-generating conformation. Thus, consistent with Ford's definition of the mechanical activation (17), A_s represents the level of mechanical activation: the number of available cross bridges in the weak conformation that can turn to the strong force-generating conformation. Calcium dissociation from troponin at T_s leads to U_s, which represents the loose-coupling concept, in which the cross bridges are still in the strong conformation but without bound calcium.

Note that the tight-coupling model (41) stipulates that calcium can dissociate from the troponin only after cross-bridge detachment; i.e., cross bridges cannot exist in the strong conformation without bound calcium on the troponin. Thus only R_s, A_s, and T_s are considered in the single-overlap region in the tight-coupling model. The proposed addition of U_s, wherein the cross bridges can exist in the strong conformation without bound calcium, assumes a loose coupling between calcium dissociation and cross-bridge weakening, hence the loose-coupling name for this model. Direct transitions from R_s to T_s or from A_s to U_s, whereby changes of cross bridges and calcium binding occur simultaneously, are neglected here.

The four analogous states in the double-overlap region are denoted R_d, A_d, T_d, and U_d. Note that the net force generated by the cross bridges in the double-overlap region is zero (36). Finally, only two states, R_n

and A_n, exist in the nonoverlap region of the filaments, corresponding to R_s and A_s in the single-overlap region.

MATHEMATICAL MODEL

Contractile element—state variable. The transitions between the troponin states are defined by the appropriate rate coefficients of calcium binding, cross-bridge cycling, or filament sliding (Table 2). The transitions between the states are bidirectional, except for the transitions from U_s to R_s and from U_d to R_d. These last transitions are unidirectional, corresponding to *assumption 7*, which stipulates that calcium is necessary for triggering ATP hydrolysis (12) and cross-bridge cycling from the weak to the strong conformation.

If the length of the effective thick myosin filament that is carrying myosin heads is L_m and the length of the single-overlap is L_s , the overlap ratio α is defined as

$$\alpha \triangleq \frac{L_s}{L_m} \quad (1)$$

where $L_m = L'_m - L_b$; L'_m is the total length of the thick myosin filament, and L_b is the length of the bare zone in the center of the thick filament.

Note that $\alpha = 1$ for maximal single-overlap length, i.e., when no double overlap exists. The sarcomere length (SL) is given by

$$SL = L_n + L_s + L_d \quad (2)$$

where L_n and L_d are the nonoverlap and double-overlap lengths (in the entire sarcomere). Under normal physi-

Table 2. *Summary of Parameters Used*

Symbol	Reported Values	Value Used	Units	Ref.
<i>Sarcomere geometry</i>				
L_a	≤ 1.25	1.15	μm	35
L'_m	1.45–1.65	1.5	μm	35
L_b	0.08–0.11	0.1	μm	35
L_z	0.08–0.16	0.1	μm	35
<i>Calcium kinetics</i>				
Troponin	60	60	μM	30
k_b	10^8	10^8	$\mu\text{M}^{-1} \cdot \text{s}^{-1}$	33
k_{-b}	0.33	0.33	s^{-1}	33
$(k_1/k_{-1})_{\text{max}}$	2×10^6	2×10^6	μM^{-1}	33
k_1	3.9×10^7	4×10^7	$\mu\text{M}^{-1} \cdot \text{s}^{-1}$	33
<i>Cross-bridge cycling</i>				
f	40	40	s^{-1}	30
g_o	11–22	12	s^{-1}	37*
	10			30
g_1		15	Dimensionless	†

Calcium currents (Eqs. 19 and 20): $[\text{Ca}]_o = 2 \text{ mM}$, $Q_s = 0.3 \text{ s}^{-1}$, $\tau_{\text{SR}} = 2 \text{ ms}$, $\tau_{\text{SF}} = 20 \text{ ms}$. $Q_o = 30 \text{ s}^{-1}$, $Q_1 = 0.6 \text{ s}^{-1}$, $\tau_{\text{IR}} = 2 \text{ ms}$, $\tau_{\text{IF}} = 100 \text{ s}$, $Q_d = 1,000 \mu\text{M} \cdot \text{l}^{-1} \cdot \text{s}^{-1}$, and $K_{\text{mu}} = 1 \mu\text{M}$. * g_o is calculated from rate of relaxation. At late isometric relaxation, free calcium concentration is low, and thus activation level (A_s) approaches zero. From Eq. 28, rate of isometric force decline is $g_o F_{\text{CE}}$. On the basis of the study of Sys and Brutsaert (37), time constant of isometric force decline is 44–85 ms; hence, $g_o = 1/0.085 \div 1/0.044 = 11 \div 22 \text{ s}^{-1}$. † Value of g_1 is based on experimentally measured (13) constant $b = 1 \mu\text{m/s}$ in Hill's equation (Eq. 31). Equation 31 then gives: $g_1 = 1/(g_o L_m)/b - 1/\alpha = 15.8 \div 14.8$, because for sarcomere length $1.6 \div 2.4 \mu\text{m}$, $\alpha = 0.5 \div 1$.

ological conditions, when the thick filament is not compressed, $SL > L'_m + L_z$, and we have

$$\begin{aligned} L_s &= \alpha L_m \\ L_d &= (1 - \alpha) L_m \\ SL &= 2L_a - L'_m + \alpha L_m + L_z \\ L_n &= SL - L'_m - L_z = 2L_a - 2L'_m + \alpha L_m - L_z \end{aligned} \quad (3)$$

where L_a is the length of the thin actin filament and L_z is the length of the z-zone. Similar equations can be written for the case of thick filament compression, where $SL < L'_m + L_z$.

The sarcomere shortening velocity V_{SL} is given by differentiating SL . Thus, from Eq. 3

$$V_{SL} = L_m V \quad (4)$$

where V is the rate of change of the overlap ratio; i.e., $V = -d\alpha/dt$.

Denoting $X_i \in \{R_n, A_n, R_s, A_s, T_s, U_s, R_d, A_d, T_d, U_d\}$, we now define \bar{X}_i as the troponin unit density (i.e., number of troponin units per unit length) of each state variable in the different overlap regions. For the isometric regimen

$$\bar{X}_i = \frac{X_i}{L_i}; \quad \bar{X}_i \in \{\bar{R}_i, \bar{A}_i, \bar{T}_i, \bar{U}_i\}; \quad i \in \{n, s, d\} \quad (5)$$

Inasmuch as the troponin units are distributed uniformly along the actin filament, the troponin density (TRo) is given by

$$\begin{aligned} \text{TRo} &= R_s + A_s + T_s + U_s \\ &= R_d + A_d + T_d + U_d = R_n + A_n \end{aligned} \quad (6)$$

and the sums of the troponin units in the single- and double-overlap regions are given by

$$\begin{aligned} \bar{R}_s + \bar{A}_s + \bar{T}_s + \bar{U}_s &= \text{TRo}/\alpha L_m \\ \bar{R}_d + \bar{A}_d + \bar{T}_d + \bar{U}_d &= \text{TRo}/[(1 - \alpha)L_m] \end{aligned} \quad (7)$$

The transition between the density state variable (\bar{X}_i) within the single overlap ($i = s$) or within the double overlap ($i = d$) is given by

$$\begin{bmatrix} \dot{\bar{R}}_i \\ \dot{\bar{A}}_i \\ \dot{\bar{T}}_i \\ \dot{\bar{U}}_i \end{bmatrix} = \begin{bmatrix} -K_1 & k_{-1} & 0 & g'_0 + g'_1 V \\ K_1 & -f - k_{-1} & g_0 + g_1 V & 0 \\ 0 & f & -g_0 - g_1 V - k_{-m} & K_m \\ 0 & 0 & k_{-m} & -K_m - g'_0 - g'_1 V \end{bmatrix} \begin{bmatrix} \bar{R}_i \\ \bar{A}_i \\ \bar{T}_i \\ \bar{U}_i \end{bmatrix} \quad (8)$$

where $K_1 = k_1[\text{Ca}]$, $K_m = k_m[\text{Ca}]$, $[\text{Ca}]$ denotes the free calcium concentration, and f , g_0 , g'_0 , g_1 , and g'_1 represent the cross-bridge turnover rate kinetics. The rate coefficients k_1 and k_{-1} represent the rate constants of calcium binding to low-affinity sites of troponin when the cross bridges are in the weak conformation; k_m and k_{-m} represent the rate constants of calcium binding when the cross bridges are in the strong conformation. Note that because the double overlap does not affect cross-bridge cycling (36) (*assumption 11*), the rate coefficients

between the density state variables are the same in the double- and single-overlap regions.

The transitions between the density state variables in the nonoverlap region are described by

$$\begin{bmatrix} \dot{\bar{R}}_n \\ \dot{\bar{A}}_n \end{bmatrix} = \begin{bmatrix} -K_1 & k_{-1} \\ K_1 & -k_{-1} \end{bmatrix} \begin{bmatrix} \bar{R}_n \\ \bar{A}_n \end{bmatrix} \quad (9)$$

Note that the rate coefficients k_{-1} and k_{-m} are not constants; the cooperative calcium binding to the regulating sites, which depends on the number of cycling cross bridges, dictates the dependence of these coefficients on the state variables (see *Cooperativity mechanism*).

On the basis of experimental evidence, two assumptions can be introduced to simplify the above equations.

1) The rate of cross-bridge weakening is independent of the existence of calcium on the troponin; $g'_0 = g_0$. This is another aspect of the loose-coupling concept. As shown by Brenner (9), a linear relationship exists between the isometric force developed in a skinned skeletal cell and the rate of ADP production. Because ADP is released during cross-bridge transition from the strong to the weak conformation, we (28) obtain that the turnover rate g' from state U_s to R_s equals the turnover rate g' from state T_s to A_s .

2) All low-affinity sites on the troponin have approximately the same apparent affinity for calcium; i.e., $k_m = k_1$ and $k_{-m} = k_{-1}$. This concept was originally postulated by Guth and Potter (20), who, using skinned rabbit psoas fiber, found the calcium affinity to be independent of sarcomere length, although the affinity increased at full activation. They attributed this phenomenon to the spread of the activation throughout the troponin-tropomyosin interaction along the entire thin filament. The synergistic effect of calcium and cross-bridge cycling in "turning on" the troponin complexes is also supported by the studies of Grabarek et al. (18) and Williams et al. (38). All these data are based on skeletal muscle. Consistently, the data of Hofmann and Fuchs (23) for the cardiac muscle also confirm this hypothesis. The affinity of the troponin for calcium does not depend on sarcomere length in the presence of vanadate (23),

which interferes with cross-bridge cycling. However, the affinity is mediated by the number of cycling cross bridges (24). In the absence of vanadate, at $SL = 2.34\text{--}2.45 \mu\text{m}$ and $\text{pCa} = 5.0$, calcium is bound to all troponin-binding sites along the filament (24) in the single-overlap and nonoverlap regions (3.2 mol calcium/mol troponin). In the presence of vanadate, at the same sarcomere length and pCa , the amount of calcium bound to troponin was significantly reduced and was almost the same as that for short sarcomere length (1.52–1.78

μm). Thus, consistent with the hypothesis of Guth and Potter (20), the cycling cross bridges in the single-overlap region affect calcium affinity in the nonoverlap region.

A change in the total amount of troponin regulatory units during contraction in each state in the single-overlap region (dX_s/dt) is determined by the changes in the density state variables ($d\bar{X}_s/dt$) of each state and by the change in the single-overlap length due to filament sliding. A sarcomere shortening of dL ($= L_m V dt$) causes a transition of segment length dL from the nonoverlap to the single-overlap region and a transition of a segment length of $2dL$ from the single- to the double-overlap region (due to the movement of the 2 actin thin filaments). The distribution of the troponin units in the segment dL that was transferred from the nonoverlap region depends on the amount of calcium bound to troponin in the nonoverlap region (described by \bar{R}_n and \bar{A}_n) and the probability of finding a cross bridge in a strong conformation in the single-overlap region.

Introducing the last assumption ($k_1 = k_m$ and $k_{-1} = k_{-m}$) yields

$$\bar{A}_s + \bar{T}_s = \bar{A}_n \quad (10)$$

Thus filament sliding does not affect the regulatory unit distribution at the edges of the single-overlap region.

Because $X_s = \bar{X}_s L_s = \bar{X}_s \alpha L_m$, we have, by differentiation, at contraction ($V > 0$)

$$\frac{dX_s}{dt} = \frac{d\bar{X}_s}{dt} \alpha L_m - \bar{X}_s L_m V \quad (11)$$

Similarly, at relaxation (sarcomere lengthening), we have

$$\frac{dX_s}{dt} = \frac{d\bar{X}_s}{dt} \alpha L_m + (2\bar{X}_d - \bar{X}_s) L_m |V| \quad (12)$$

Similar equations are derived for the double-overlap and nonoverlap regions. Note that the second item on the right-hand side of *Eqs. 11 and 12* represents the mathematical interpretation of *assumption 14*.

Bound calcium and force. The total amount of calcium bound to the low-affinity sites (BCa_L) is given by

$$BCa_L = A_s + T_s + A_d + T_d + A_n \quad (13)$$

The kinetics of calcium binding to the high-affinity sites (BCa_h), based on *assumption 6*, is given by

$$\frac{d(BCa_h)}{dt} = (2TRo - BCa_h)[Ca]k_h - BCa_h k_{-h} \quad (14)$$

Although the high-affinity sites do not regulate cross-bridge cycling, they have some effect on the free calcium transient. As shown by Robertson et al. (33), the high-affinity sites play a significant role when the performance of the cardiac muscle is analyzed in response to changes in the excitation rate. Here, a steady excitation rate is assumed to calculate the initial amount of calcium bound to the high-affinity sites.

The force (F) generated by the sarcomere is proportional to the sum of states T_s and U_s in the single-overlap

region. The rate of cross-bridge attachment and detachment is at least an order of magnitude faster than the rate of cross-bridge cycling between the weak and the strong conformation. The rate constants of attachment and detachment in Huxley's model are of the order of $1-40 \text{ s}^{-1}$ (41), whereas according to Brenner (8), the rate of detachment of the cross bridges in the strong conformation is $50-1,000 \text{ s}^{-1}$ and the attachment rate is at least an order of magnitude larger than the detachment rate. Thus the relatively slow rate constants used in Huxley's model for simulating muscle contraction (39, 41) characterize the cross-bridge cycling between the weak and the strong conformations, rather than the rate of attachment and detachment (8). Consequently, the relatively slow ATP hydrolysis is linked to cross-bridge cycling from the weak to the strong conformation (10, 16), rather than to the attachment or detachment phenomena. Moreover the cross bridges in the strong conformation can detach and reattach several times per ATP hydrolysis (31).

The present model describes the rate-limiting processes that are related to cross-bridge cycling between the weak and the strong conformation and assumes that the cross bridges reach equilibrium between attachment and detachment quite rapidly relative to the rates of transition between the weak and the strong conformation.

According to *assumption 15*, the average generated force per cross bridge is given by

$$F_{CB} = \bar{F} - \eta V \quad (15)$$

where \bar{F} is the unitary force developed by each cross bridge at isometric contraction and η represents the viscous element property of the single cross bridge (14).

The force generated by the cross bridges (F_{CE}) per unit filament cross section is given by

$$F_{CE} = (T_s + U_s)(\bar{F} - \eta V) = \alpha L_m (\bar{T}_s + \bar{U}_s)(\bar{F} - \eta V) \quad (16)$$

The internal load is simulated here by the parallel element (Fig. 1), which has viscous properties (14) and a passive elastic property (5)

$$F_{PE} = \begin{cases} E(e^{D(SL/Sp_0-1)} - 1) + \eta_{PE} V_S & (SL \geq Sp_0) \\ -B \left(1 - \frac{SL}{Sp_0}\right) + \eta_{PE} V_{SL} & (SL < Sp_0) \end{cases} \quad (17)$$

where SL is given in *Eq. 3*, Sp_0 is the length of the unstressed sarcomeres, E , D , and B are empirical constants (5), and η_{PE} represents the viscous property of the internal load. The total force per unit filament cross section is given by

$$F = F_{CE} + F_{PE} \quad (18)$$

Cooperativity mechanism. The positive-feedback mechanism, denoted as cooperativity, is based on our previous analysis of skinned cell data and is described extensively elsewhere (28). Hofmann and Fuchs (24) measured the force and the bound calcium, with and without vanadate, at different free calcium concentra-

tions and sarcomere lengths in skinned cardiac muscle. The total amount of bound calcium in the presence of vanadate is independent of sarcomere length (23), whereas the amount of bound calcium is force dependent in the absence of vanadate (24). Hibberd and Jewell (21) and Kentish et al. (26) measured the force-length-free calcium relationship in the skinned cardiac muscle. Analysis of these data by us (28) suggests that the dominant cooperativity mechanism in the cardiac cell results from the dependence of the affinity of troponin for calcium on the number of cycling cross bridges, whereas the free calcium concentration and the sarcomere length have a negligible effect on the apparent calcium-binding coefficient. The reported length-dependent calcium sensitivity (1) is actually mediated by the number of cross bridges in the strong conformation. Increasing the sarcomere length increases the number of available cycling cross bridges, thus increasing calcium affinity. The increase in the bound calcium further increases the number of cross bridges in the strong conformation. Thus the cooperative mechanism affects the FLR and may therefore contribute to understanding the Frank-Starling law (1).

The study of Kentish et al. (26) demonstrates that the shape of the FLR for the intact cardiac muscle resembles that of the FLR for the same skinned muscle. Thus the same mechanism postulated in the skinned cell exists in the intact cell.

The rate constant of calcium binding to troponin, taken here as a constant, $k_1 = 40 \times 10^6$, is based on the study of Robertson et al. (33). The dependence of K on the number of cross bridges is described in Fig. 3, on the

basis of our earlier study (28) of the skinned cell. The maximal magnitude of the calcium affinity is taken as $K_{max} = 2 \times 10^6$, in accordance with Robertson et al. The affinity of troponin for calcium is defined as $K = k_1/k_{-1}$. Thus the rate constant of calcium dissociation from the troponin, k_{-1} , is calculated as follows: $k_{-1} = k_1/K$.

The intact and the skinned muscle differ in the magnitude of the calcium affinity: the calcium affinity is far greater in the intact cell than in the skinned cell (40). Note that using the relationship given in Fig. 3 yields the force-pCa relationship for the intact cell (not shown here) reported by Yue et al. (40).

No analytic solution could be found for the set of nonlinear differential equations representing the general case, where the coefficients of the equation, which depend on the free calcium concentration, are time variant. Thus the solution for the general case is obtained by numerical procedures with use of the fourth-order Runge-Kutta method (commercially available in MATLAB). The program runs on a fast IBM-compatible PC.

Calcium transport. To simulate the free calcium transients, we have used a simple phenomenological model of the sarcolemmal and sarcoplasmic reticulum (SR) calcium currents (Fig. 1), which is based on the model of Lee and Allen (30). The calcium currents through the sarcolemma and the SR are given as a deterministic function of the extracellular calcium and the intra-SR calcium content. No interaction between the sarcolemma and the SR is assumed. The inward calcium current (I_s) due to the action potential is represented by (30)

$$I_s = Q_s((1 - e^{-t/\tau_{SR}}) e^{-t/\tau_{SF}} + I_l)[Ca]_o \quad (19)$$

where $[Ca]_o$ is the extracellular calcium concentration, Q_s is the maximal permeability of the sarcolemma; τ_{SR} and τ_{SF} represent the time constants of rise and decline of the inward calcium current, respectively, and I_l represents leak current. I_o denotes a first-order efflux of calcium through the sarcolemma (i.e., $I_o = Q_o[Ca]$), which represents the Na/Ca exchanger.

The calcium release from the SR, denoted I_i , is described by an equation identical to Eq. 19, but with Q_i , τ_{iR} , τ_{iF} , and $[Ca]_r$ replacing Q_s , τ_{SR} , τ_{SF} , and $[Ca]_o$, respectively. $[Ca]_r$ represents the available free calcium in the releasing terminal of the SR, Q_i is the maximal permeability, and τ_{iR} and τ_{iF} denote the rise and decline time constants, respectively. Calcium sequestration into to the SR, I_u , is given by the Michaelis-Menten equation

$$I_u = Q_u[Ca]/(K_{mu} + [Ca]) \quad (20)$$

where Q_u is the maximal pumping rate and K_{mu} is the Michaelis-Menten constant representing the free calcium concentration at one-half the pumping rate.

RESULTS

FLR. Figure 4 depicts isometric contractions at different sarcomere lengths. The simulation shows the force (Fig. 4A) and the free calcium (Fig. 4B) in the first

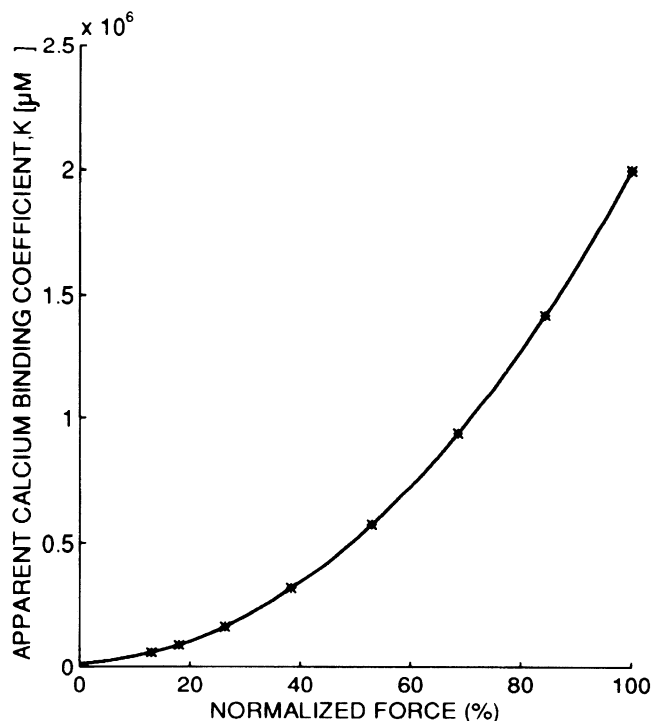


Fig. 3. Dependence of affinity of troponin for calcium (K) on no. of cycling cross bridges. No. of cycling cross bridges is described by normalized isometric force.

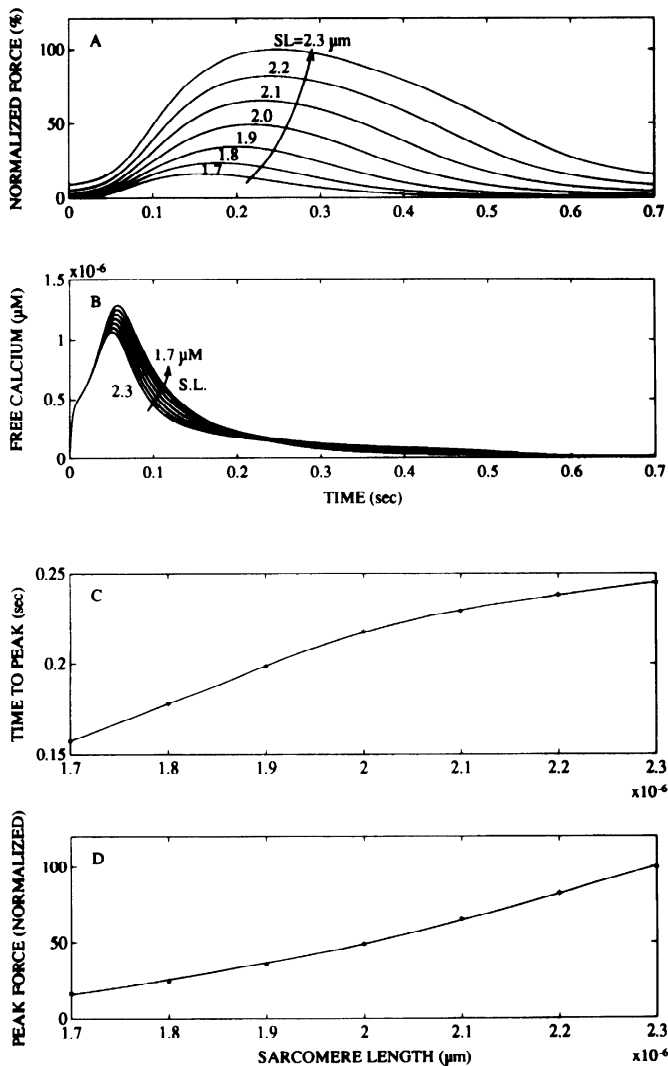


Fig. 4. Simulation of isometric contraction for different muscle lengths. *A*: normalized force. *B*: 1st free calcium transient obtained after muscle length shortening corresponding to data of Allen and Smith (4). *C*: time to peak force at different sarcomere lengths. *D*: force-length relationship. $[Ca]$ is normalized relative to peak $[Ca]$ at maximal sarcomere length (SL_{max}). Force is normalized by peak force at SL_{max} .

contraction after change in the sarcomere length. The results reveal three phenomena due to the cooperativity mechanism. Figure 4*B* demonstrates an increase in the first free calcium transient after sarcomere length shortening, corresponding to the data of Allen and Smith (4). Figure 4*C* shows that the time to peak force increases with the increase in the sarcomere length, as was postulated experimentally by Allen and Kurihara (3). Finally, in agreement with Allen and Kentish (1), Fig. 4*D* shows the simulated peak FLR in the intact cardiac cell. Note that this relationship is different from that obtained for the skeletal muscle (1).

The calculated effect of changing $[Ca]_o$ on the FLR of the first contraction after change in $[Ca]_o$ is shown in Fig. 5. Consistent with reported experimental data (1), the FLR shifts to the right when $[Ca]_o$ is reduced. As shown by Allen and Kentish (1), there is a difference between the FLR for the first beat after change in $[Ca]_o$

and the FLR for the steady state after several beats, which is shifted farther to the right. Note that the present study simulates only the first beat after the length change. The steady-state FLR depends greatly on the control of the calcium transient and the interaction between calcium current through the sarcolemma and the SR and on the mechanism of calcium-induced calcium release and the calcium content of the SR. This point is beyond the scope of the present study.

Figure 6 demonstrates the calculated effect of changing the maximal affinity of troponin for calcium. Increasing the affinity shifts the FLR to the left. These results indicate that the FLR is determined by the cooperativity feedback, which affects the mechanical activation level, represented here by state A_s .

As shown in Figs. 5 and 6, interventions that raise the free calcium or increase calcium binding to troponin elevate the activation level (state A_s), shift the FLR curve to the left, and affect its steepness. The reported length-dependent sensitivity to calcium (1) can thus be explained by the positive-feedback mechanism of the cooperativity: an increase in the sarcomere length increases the number of available cross bridges in the single-overlap region, thus increasing the activation level, state A_s . Elevation of the activation increases the number of cross bridges in the strong conformation and, through the cooperativity mechanism, further elevates calcium affinity.

Figure 7 illustrates the FLR at isometric and isotonic contractions. The sarcomere length is determined as the length at the end of shortening for the isotonic contraction (25). Starting from the same initial length, the end-shortening points of the isotonic contractions with

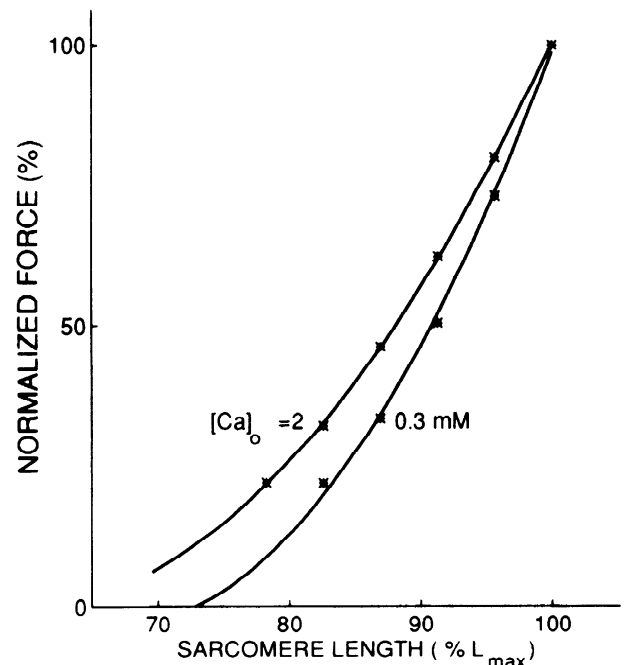


Fig. 5. Force-length relationship at different extracellular calcium concentrations ($[Ca]_o$) corresponding to data of Allen and Kentish (1). Data points were calculated by model simulation. Note that increasing $[Ca]_o$ shifts force-length relationship to left and reduces its steepness.

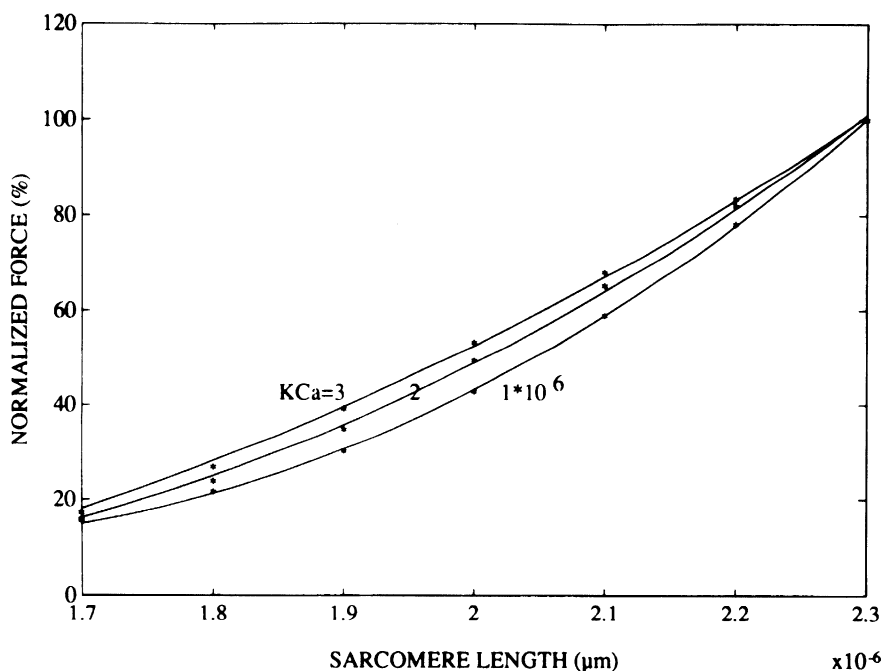


Fig. 6. Force-length relationship for different affinities of troponin for calcium (K_{Ca}). Data points were calculated by model simulation. Note that increasing affinity of troponin for calcium shifts force-length relationship to left.

different isotonic loading levels fall essentially on a single end-shortening force-length curve. This curve of the isotonic contractions is to the right of the curve derived on the basis of the isometric contractions, in accordance with the experimental study of Izakov et al. (25). This shift is due to the effect of the mechanical feedback: increasing the velocity of shortening increases the rate of cross-bridge turnover from the strong to the weak conformation.

FVR and Hill's equation. The FVR has been defined in the literature at different mechanical settings: the maximal velocity at isometric-isotonic changeover experiment (7), the velocity measured after quick release to a constant load (13), or slower release at a controlled

velocity of shortening (13). By using a laser differentiation method to measure the sarcomere length, Daniels et al. (13) obtained identical FVRs in their experiments with quick release and with release at a constant velocity of shortening. Their FVR fits the well-known Hill's "law" (22)

$$(F_0 - F)b = (F + a)V_{SL} \quad (21)$$

where F_0 is the maximal isometric force level and a and b are experimentally determined constants.

The FVR is now calculated here analytically, on the basis of the quick release to a constant-load experimental procedure. By use of *Eqs. 16-18*, the rate of force

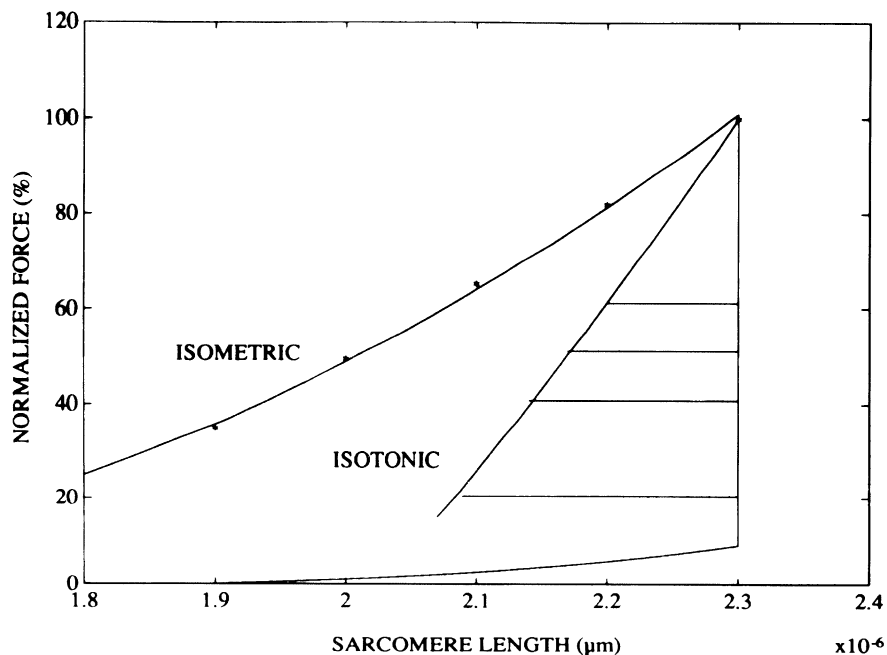


Fig. 7. Force-length relationships at isometric and isotonic contractions. Sarcomere length is defined as length at end of shortening for isotonic contraction. Note shift to right of end-shortening force-length relationship relative to that based on isometric contractions.

development is given by

$$\frac{dF}{dt} = (\bar{F} - \eta V) \cdot \frac{d(T_s + U_s)}{dt} - (T_s + U_s)\eta\dot{V} - K_{PE}V - \eta\dot{V} \quad (22)$$

where $T_s + U_s = (\bar{T}_s + \bar{U}_s)\alpha L_m$ and K_{PE} , the elastic element of the internal load, is given by

$$K_{PE} = \left. \frac{dF_{PE}}{d\alpha} \right|_{\eta_{PE}=0} = \begin{cases} \frac{EDL_m}{Sp_0} e^{D(SL/Sp_0-1)} & (SL \geq Sp_0) \\ \frac{BL_m}{Sp_0} & (SL < Sp_0) \end{cases} \quad (23)$$

By use of Eqs. 8 and 11, Eq. 22 is written as

$$\begin{aligned} \frac{dF}{dt} = & (\bar{F} - \eta V)[f\bar{A}_s\alpha L_m \\ & - (g_0 + g_1 V)(\bar{T}_s + \bar{U}_s)\alpha L_m \\ & - (\bar{T}_s + \bar{U}_s)L_m V \\ & - K_{PE}V - [\eta\alpha L_m(\bar{T}_s + \bar{U}_s) + \eta_{PE}]\dot{V} \end{aligned} \quad (24)$$

Introducing Eq. 16 for the contractile element force in Eq. 24 gives

$$\begin{aligned} \frac{dF}{dt} = & f\bar{A}_s\alpha L_m(\bar{F} - \eta V) - \left(g_0 + g_1 V + \frac{V}{\alpha}\right) F_{CE} \\ & - K_{PE}V - [\eta\alpha L_m(\bar{T}_s + \bar{U}_s) + \eta_{PE}]\dot{V} \end{aligned} \quad (25)$$

Rearranging Eq. 25, we obtain

$$\begin{aligned} \frac{dF}{dt} = & \bar{F}fA_s - g_0F_{CE} \\ & - \left[\left(g_1 + \frac{1}{\alpha}\right)F_{CE} + \eta fA_s + K_{PE}\right]V \\ & - [\eta\alpha L_m(\bar{T}_s + \bar{U}_s) + \eta_{PE}]\dot{V} \end{aligned} \quad (26)$$

where $A_s = \bar{A}_s\alpha L_m$.

At constant load or isotonic contraction ($dF/dt = 0$), the sarcomere shortening velocity stabilizes ($\dot{V} = 0$). Using Eq. 3, we obtain

$$V_{SL_{isotonic}} = \frac{\bar{F}fA_s - g_0F_{CE}}{\left(g_1 + \frac{1}{\alpha}\right)F_{CE} + \eta fA_s + K_{PE}} \cdot L_m \quad (27)$$

The velocity of shortening thus depends on state A_s , the level of activation, and on f , the rate of cross-bridge turnover from the weak to the strong conformation, and is inversely related to the internal load stiffness, K_{PE} . The quick release to constant-load experiments is performed from isometric contraction (13, 15). For isometric contraction, $V = 0$, and Eq. 26 yields

$$\frac{dF_{CE}}{dt} = \bar{F}fA_s - g_0F_{CE_m} \quad (28)$$

where F_{CE_m} is the force generated at isometric contraction.

At peak isometric contraction ($F_{CE} = F_{CE_0}$), $dF/dt = 0$ and Eq. 28 reduces to

$$\bar{F}fA_s = g_0F_{CE_0} \quad (29)$$

The FVR is measured by quick release from the peak isometric point to a constant-load level. The peak isometric point thus defines the intercept of the force-velocity curve with the force axis ($V_{SL} = 0$, $F_{CE} = F_{CE_0}$). Equation 29 allows us to approximate the level of activation A_s in Eq. 27 from the activation level before the quick release. Substituting Eq. 29 into Eq. 27 gives

$$V_{SL} = \frac{g_0L_m}{\left(g_1 + \frac{1}{\alpha}\right)} \frac{(F_{CE_0} - F_{CE})}{\left(F_{CE} + \frac{K_{PE} + \eta fA_s}{g_1 + \frac{1}{\alpha}}\right)} \quad (30)$$

The change of the sarcomere length during the quick release is always $< 2\%$ of the initial sarcomere length (13), indicating that the change in the parallel element of force is relatively small. Introducing Eq. 18 into Eq. 30 gives

$$V_{SL} = b \frac{F_0 - F}{F + a}$$

or, in the more familiar Hill's form

$$b(F_0 - F) = (F + a)V_{SL} \quad (31)$$

where

$$a = (K_{PE} + \eta fA_s)/(g_1 + 1/\alpha) - F_{PE}$$

$$b = (g_0L_m)/(g_1 + 1/\alpha)$$

Equation 31 is identical to the classic Hill equation (Eq. 21) and provides the physiological meaning to the previously experimentally determined constants a and b . Thus the derivation of Hill's equation based on physiological considerations suggests that the FVR is not an independent constitutive property of the muscle. Note that Eq. 31 is obtained here once we make the assumption that the rate of cross-bridge weakening depends linearly on the filament-sliding velocity.

The velocity of sarcomere shortening at any level of activation in the isotonic regimen is given by Eq. 27. Furthermore, Hill's equation (Eq. 31) was derived here analytically by use of the quick-release experimental method. The versatility of the model is further demonstrated in Fig. 9 by simulation of the FVR, obtained by the isometric-isotonic changeover method (Fig. 8), as performed by Braunwald (7). Some of the isotonic contractions that were used to derive the FVR, at an initial sarcomere length of 2.3 μm , are shown in Fig. 8. The maximal velocities of shortening during the isometric-isotonic changeover at various isotonic loadings were used to construct the FVRs. Figure 9 also demonstrates the effect of initial muscle length on the FVRs.

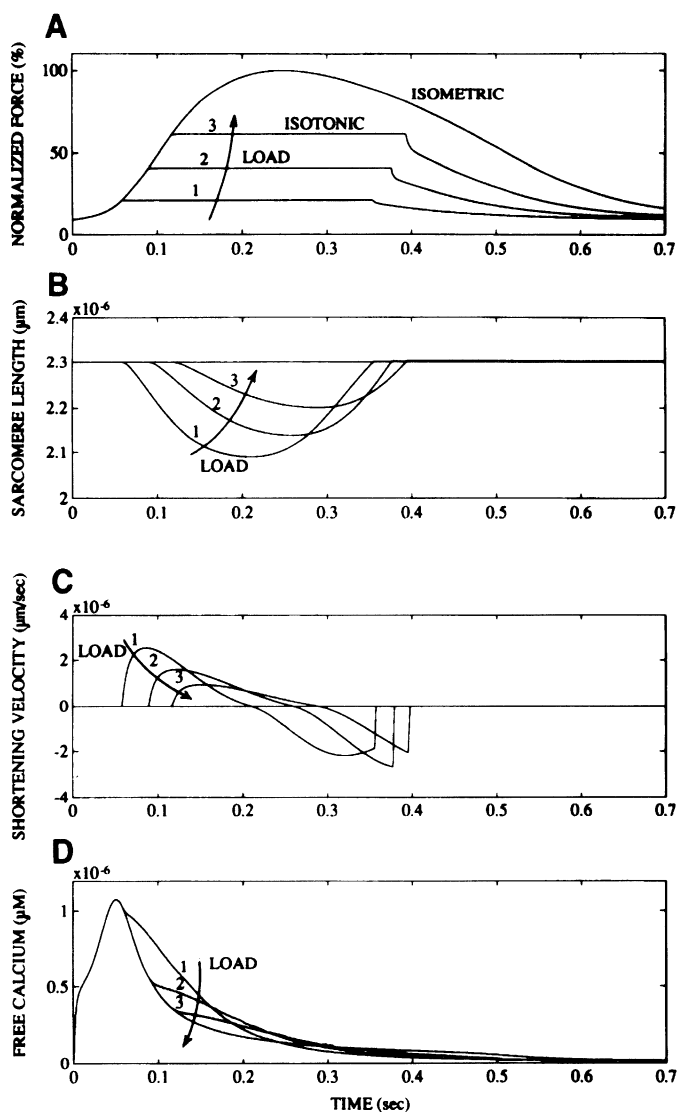


Fig. 8. Load dependence of relaxation. A: normalized force for different levels of isotonic loading. B: sarcomere lengths; note reduction in contraction duration when load is reduced, corresponding to measurements of Brutsaert et al. (11). C: sarcomere shortening velocity. D: free calcium transient is reduced as load is increased, corresponding to data of Lab et al. (27).

Inspection of the simulation results reveals also the disadvantage of the FVR derived from isometric-isotonic contraction; i.e., the activation level is not uniform at the various instants of measuring the shortening velocity, and consequently the FVR is underestimated by this method.

It is important to note that no attempt is made here to achieve precise parameter estimation to Braunwald's experiments (7). This is due to the absence of a unique parameter set, because Braunwald's measurements were performed on a papillary muscle without precise measurements of the sarcomere lengths; thus the effect of the serial elasticity due to the damaged ends and the degree of intrafiber ischemia are not known. Moreover the calcium transient was not measured.

Contrary to earlier models of cardiac muscle contraction (5, 25), where the FVR was considered a constitu-

tive law of the muscle, the shortening velocity here is a function of the activation level during contraction.

Unloaded velocity. The unloaded velocity, V_u , for an unloaded sarcomere shortening is obtained from Eq. 27 and is given by

$$V_u = \frac{\bar{F}L_m f\bar{A}_s L_s}{\eta f\bar{A}_s L_s + K_{PE}} = \frac{\bar{F}}{\eta} L_m \frac{1}{1 + \frac{K_{PE}}{\eta f\bar{A}_s L_s}} \quad (32)$$

where $L_s = \alpha L_m$. Equation 32 states that the maximal unloaded sarcomere velocity depends on 1) the level of activation, \bar{A}_s , as stipulated by Zahalak and Shi-ping (41) and Daniels et al. (13), 2) the rate of cross-bridge cycling from the weak to the strong conformation, f , as stipulated by Brenner and Eisenberg (10), and 3) the inverse of the stiffness of the internal load, K_{PE} , consistent with the findings of Ford (17).

Equation 32 indicates that the unloaded velocity depends on the single-overlap length (L_s ; or, equivalently, sarcomere length) and on the activation level \bar{A}_s or indirectly on the free calcium level. Increasing the sarcomere length (and thus increasing L_s) or the free calcium level (and thus \bar{A}_s) elevates the unloaded velocity. These predictions are in accordance with the measurements of de Tombe and ter Keurs (14).

For a high level of activation, when $\eta f\bar{A}_s L_s \gg K_{PE}$, Eq. 32 is reduced to yield the following expression for the maximal unloaded velocity

$$V_{max} = \frac{\bar{F}}{\eta} L_m \quad (33)$$

Equation 33 is consistent with the measurements of Edman (15) and Daniels et al. (13), which show that the maximal unloaded velocity of shortening is constant in the sarcomere length range of 1.65–2.7 μm (15) at high levels of activation.

With use of the expressions for the maximal unloaded velocity (Eq. 33) and the activation level at peak isometric force (Eq. 29), Eq. 32 gives

$$V_u = V_{u_{max}} \frac{F_{CE_0}}{F_{CE_0} + C} \quad (34)$$

where F_{CE_0} is the peak isometric force generated by the contractile element and C is constant, given by $C = K_{PE} V_{u_{max}} / g_0 L_m$.

Equation 34 for the unloaded velocity is identical to the equation proposed by de Tombe and ter Keurs (14) on the basis of their experimental data. Note that unlike that reported by de Tombe and ter Keurs, the activation level in the present study is not defined as the isometric force. Moreover, we can distinguish between the effect of the single-overlap length and the effect of the activation level on the unloaded shortening velocity.

Force deficit. Using an isolated papillary muscle of a rabbit, Leach et al. (29) measured the effect of constant shortening velocity on the developed force. They compared the force generated at various shortening velocities and times of contraction with the force predicted

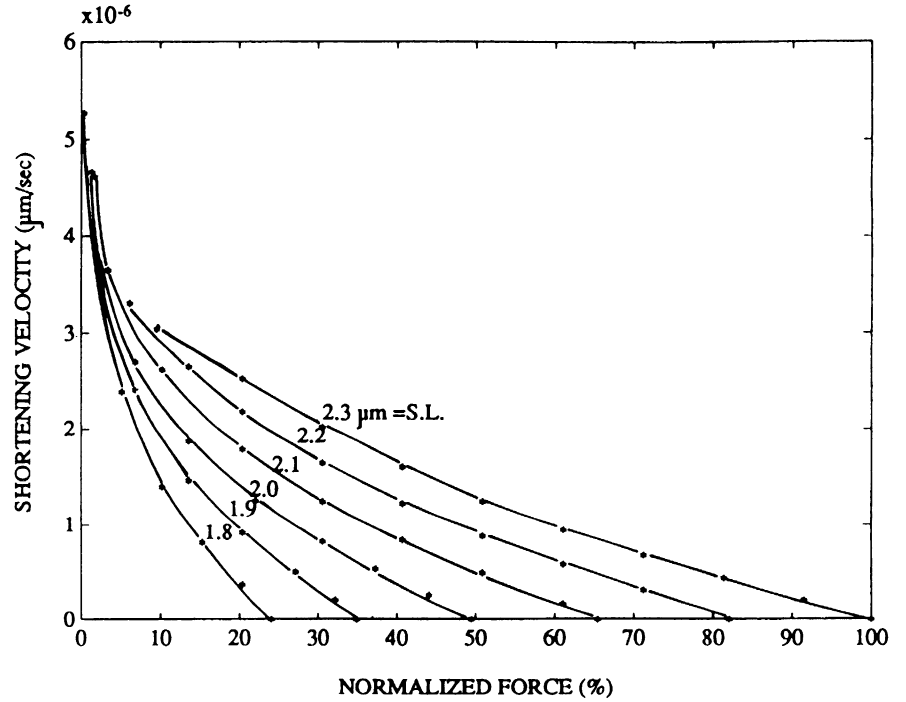


Fig. 9. Force-velocity relationships for different sarcomere lengths calculated from simulation of isometric-isotonic changeover experiments, shown in Fig. 8, performed by Braunwald (7). Data points were calculated by model simulation. Simulation demonstrates importance of activation and internal load.

from measurements of isometric contractions at the same instantaneous muscle length and duration of contraction. They demonstrated that the difference, "force deficit," between the shortening force (F) and the predicted force based on isometric contractions (F_m) depends on the shortening velocity and the duration of shortening. On the basis of their study, Sagawa et al. (34) derived a linear relationship between the force deficit ($F_m - F$) and the shortening velocity

$$(F_m - F) \propto mVF_m \quad (35)$$

where m is an experimental constant that was found to increase linearly with time.

For constant velocity of shortening (i.e., $\dot{V} = 0$), the rate of force generation is derived from Eq. 26 and takes the form

$$\frac{dF}{dt} = \bar{F}fA_s - g_oF_{CE} - \left[\left(g_1 + \frac{1}{\alpha} \right) F_{CE} + \eta fA_s \right] V \quad (36)$$

because, for the experiment of Leach et al. (28), $K_{PE(t)} \ll (g_1 + 1/\alpha)F_{CE}$. The rate of isometric force generation at time t , $F_m(t)$, is then

$$\frac{dF_m(t)}{dt} = \bar{F}fA_s(t) - g_oF_m(t) \quad (37)$$

and at time $t + \Delta t$, the isometric force is

$$F_m(t + \Delta t) = F_m(t) + [\bar{F}fA_s(t) - g_oF_m(t)]\Delta t \quad (38)$$

The shortening force at the same instant is now given by

$$F(t + \Delta t) = \{F_m(t) + [\bar{F}fA_s(t) - g_oF_m(t)]\Delta t\} - \left[\left(g_1 + \frac{1}{\alpha} \right) F_m(t) + \eta fA_s(t) \right] V\Delta t \quad (39)$$

The first term on the right-hand side of Eq. 39 is equivalent to the isometric force at time $t + \Delta t$. Thus Eq. 39 can be approximated to give

$$F(t) \approx F_m(t) - \left(g_1 + \frac{1}{\alpha} \right) \Delta t V F_m(t) \quad (40)$$

because, by Eq. 31

$$\eta fA_s(t) < (a + F_{PE}) \left(g_1 + \frac{1}{\alpha} \right) \ll F_m(t) \left(g_1 + \frac{1}{\alpha} \right) \quad (41)$$

where a is the Hill coefficient. On the basis of the measurement of Daniels et al. (13), a is approximately equal to 10% of the isometric force. Hence, for the experimental conditions of Leach et al. (29), where the changeover from isometric contraction to the constant-velocity shortening was at approximately one-half of the peak isometric force, $\eta fA_s(t)$ is negligible relative to $(g_1 + 1/\alpha)F_m$.

Consistent with the analysis of Sagawa et al. (34), Eq. 40 indicates that the generated force is affected by the velocity of sarcomere shortening (V) and the duration of shortening (Δt) (34). Moreover Eq. 40 also predicts that, as suggested by Sagawa et al. (34), the force deficit ($F_m - F$) is proportional to the force level.

Clearly, the linear dependence of the force deficit on the shortening velocity and its dependence on the force level, as experimentally determined by Leach et al. (29) and Sagawa et al. (34) and theoretically by Eq. 40, strengthen the assumption that the rate of cross-bridge weakening is linearly dependent on the shortening velocity.

Load-dependent relaxation and free calcium transients. Brutsaert et al. (11) demonstrated the phenomenon of load-dependent relaxation. They showed that

the transition from the isotonic to the isometric phase in the cardiac muscle of a normal cat occurs earlier when the load is reduced. The simulation of isotonic contractions (Fig. 8) depicts this phenomenon, which is attributed to the mechanical feedback, whereby the filament-sliding velocity affects cross-bridge cycling. Load reduction increases the velocity of shortening (Fig. 8C), which in turn increases the rate of cross-bridge turnover to the weak conformation; the higher the velocity of filament sliding, the faster is the onset of relaxation.

Figure 8D demonstrates the influence of the mechanical loading conditions on the free calcium transient. As experimentally shown by Lab et al. (27), the calculated calcium transient in the isotonic contraction is wider than that in the isometric contraction. Moreover the free calcium transient in the isotonic contractions is wider when the load is reduced. This is due to the mechanical feedback and the cooperativity mechanism.

The simulations show the effect of different mechanical conditions on the bound and free calcium. In particular we note the following.

1) The free calcium is elevated in the first isometric contraction, after length shortening. This phenomenon is shown in Fig. 4B and is in accordance with the data of Allen and Smith (4). Moreover the simulations are in agreement with those of Allen and Kurihara (3), who demonstrated a wider free calcium transient at isometric contraction for a short than for a long sarcomere length.

2) The free calcium transient is elevated more in the isotonic than in the isometric contraction (Fig. 8D). As also measured by Lab et al. (27), the reduction of the load in isotonic contraction elevates the free calcium.

DISCUSSION

The study couples the kinetics of calcium binding to the low-affinity sites of the troponin regulatory units with the kinetics of cross-bridge turnover. The analysis is based on a biochemical model of cross-bridge cycling and troponin-tropomyosin regulation. Relatively simple assumptions are used here to simulate the role of troponin in regulating muscle activity and in characterizing the activation function. Whereas the model is shown to describe the various stages of the cardiac contraction, this presentation concentrates mainly on the FVR: it emphasizes that the FVR and, hence, the unloaded velocity and the shortening deactivation are not a constitutive law of the muscle but can be described on the basis of a physiological quantitative description of cross-bridge cycling and calcium kinetics.

One major difficulty in the analysis of the cardiac muscle performance is the description of the transient processes that take place in the myocytes. The free calcium in the intact cell is never at a steady state; hence, the mechanical activation function varies with time. The FLR and the FVR depend on the level of activation (17) and on the mechanical constraints. Therefore, adequate characterization of the transient activation function is crucial for the simulation of the cardiac muscle performance. We define the level of activation as the number of available cross bridges at the weak con-

formation that can turn to the strong force-generating conformation in the single-overlap region, which is described here by state A_s. This definition enables us to successfully describe the FLR and FVR at various mechanical conditions and calcium concentrations.

Cooperativity mechanism. The model uses only the type of cooperativity that is related to the effect of the number of cross bridges in the strong conformation on the apparent calcium-binding coefficient, with the assumption that this positive-feedback cooperativity mechanism is the dominant feedback mechanism that regulates calcium binding to troponin. The application of this type of cooperativity is based on our analysis of the force-length-free calcium relationships in the skinned cell and on the measured data of bound calcium to troponin (28). Obviously, the free calcium concentration in skinned cell experiments is steady, in contrast to that in the intact muscle, where the free calcium concentration has a brief transient. Moreover, because of changes in the concentration of various cytoplasmic metabolites and changes in intracellular processes, it is reasonable to expect that the performance of the skinned cell will differ from that of the intact muscle. However, the contractile proteins of the skinned and intact muscle are similarly controlled by the regulatory proteins (Fig. 1), and therefore the cooperativity mechanism is the same in both, although its magnitude can differ.

As is well known, the muscle employs an adaptive control mechanism, and different mechanical responses are generated when the parameters of the control system and the free calcium concentration transient are changed. This adaptive control mechanism plays a central role when the affinity of troponin to calcium varies as a result of inotropic stimulation or changes in the intracellular pH. Kentish et al. (26) reported that the shapes of the FLRs are similar in the intact cell and the (same) skinned cell, although they were obtained at different intracellular and extracellular calcium concentrations. Their study strengthens the idea that the same regulatory mechanism of the contractile regulatory proteins determines the performances of the skinned and intact cell. Thus we believe that the skinned cell studies can be used to characterize the control mechanism and, especially, the cooperativity mechanism.

Izakov et al. (25) suggest a model with two types of cooperativity mechanisms and define the cooperativity of the first type as the dependence of the affinity of troponin for calcium on the conformation of the cross bridge in the vicinity of the troponin. The cooperativity described in the present model links the affinity of troponin for calcium to the total amount of cross bridges at the strong conformation in the filament. The global effect of the cross bridges on calcium affinity is based here on the analysis of the amount of calcium bound to troponin at various length, force, and free calcium levels. This concept is in accordance with the findings of Guth and Potter (20), who suggest the existence of a global effect: the entire filament can be activated by a small number of cross bridges at the edge of the filament. The studies of Grabarek et al. (18) and Williams et al. (38) also support the interaction among the

troponin-tropomyosin units. Moreover the study of Brandt et al. (6) also supports the hypothesis of Guth and Potter that the activation propagates along the filament through the troponin-tropomyosin interaction; they propose that all 26 troponin-tropomyosin units along the thin filament are activated cooperatively. Izakov et al. (25) describe this global effect in their second type of cooperativity, defined as an increase in the affinity of troponin to calcium when calcium is bound to a neighboring troponin. The question is whether the cooperativity mechanism with the "global" effect is due to cross bridges at the strong conformation or to calcium binding to neighboring troponin.

Guth and Potter (20) showed that the cooperativity of calcium binding to troponin is lost in the absence of ATP. Hofmann and Fuchs (23), using a cardiac muscle, demonstrated a remarkable reduction of the calcium bound to troponin in the presence of vanadate. Thus it seems that the effect of the cooperativity is mainly due to the interaction of cycling cross bridges with the thin filaments. Moreover, Williams et al. (38) demonstrated that calcium alone cannot fully activate the ATPase, but cross-bridge binding increases the activity of ATPase by ~10-fold.

The model of Izakov et al. (25) used Hill's equation as a constitutive law of the muscle for any level of activation and time during the contraction. In contrast, Hill's equation is derived analytically (Eq. 28) and is an implicit property of the present model.

Another fundamental difference between the present model and the study of Izakov et al. (25) relates to the calculation of the generated force. They assume (their Eq. 1) that the generated force is the product of the average force of a single cross bridge, the amount of calcium troponin complexes, and the probability that a cross bridge will be attached to the thin filament. Thus the activation function of their model is equivalent to the amount of bound calcium, independent of whether the adjacent cross bridges are attached or detached. This definition of the activation function implies a tight coupling between calcium kinetics and cross-bridge cycling: cross bridges generate force only when calcium is bound to troponin, and when no calcium is bound to troponin the force is zero. Peterson et al. (32) studied the rate of isometric force development after quick release at various instants during the twitch and suggested that the bound calcium decays well ahead of the force decay. Thus the cross bridges at late relaxation generate force, although the amount of bound calcium is negligible.

Tight and loose coupling. Zahalak and Shi-ping (41) introduced the terms "tight" and "loose" couplings to describe the relationship between calcium kinetics and cross-bridge turnover in the skeletal muscle. Zahalak and Shi-ping adopted the tight-coupling model and argued that loose coupling cannot describe the extra calcium release observed in quick-release experiments. However, the tight-coupling concept requires the very rigorous assumption that calcium can release from the low-affinity sites only after the detachment of the cross bridges. Conversely, introducing adaptive coefficients in

the loose-coupling model, so that the apparent calcium-binding coefficient to the low-affinity sites becomes a function of the developed force, can explain the extra calcium release observed in quick-release experiments: quick release reduces the number of cross bridges at the strong conformation and causes a reduction in the affinity to calcium, resulting in extra calcium release from the binding sites.

The theoretically generated changes in the free calcium transients at various mechanical conditions (Figs. 4B and 8D) fit the experimentally observed changes, as measured using aequorin (3, 4, 27). These changes include the elevation of calcium transients after isotonic contraction compared with isometric contraction (27), the increase in the first free calcium transient after length shortening (4) before the contraction, and the wider free calcium transient at shorter sarcomere length (3).

Weak and strong conformations and cross-bridge attachment and detachment. According to the biochemical models of muscle contraction (16), the process of cross-bridge cycling between the strong and the weak conformations is due to nucleotide binding and release: states actin-myosin-ATP and actin-myosin-ADP-phosphate correspond to weakly bound cross bridges, whereas when ADP is associated with the myosin without phosphate, the cross bridges are at the strong force-generating conformations (16). Therefore, ATP hydrolysis and phosphate dissociation are related to the transition of the cross bridges from the weak to the strong conformation (10).

There are biochemical studies showing that the myosin-ATP, the weak conformation, attaches and detaches from actin very rapidly. Moreover, Lombardi et al. (31) and Brenner (8) postulated that even when the cross bridges are in the strong conformation, there is evidence of rapid cross-bridge attachment and detachment between the myosin and actin filaments.

The rate constants of "mechanical" attachment/detachment are much faster than the rate constants of cross-bridge cycling (8); thus the cross bridges approach equilibrium between attachment and detachment within the time course of cross-bridge cycling between the strong and the weak conformation. The present study describes the rate-limiting processes (*assumptions 3 and 4*) associated with cross-bridge cycling between the weak and the strong conformation. The average force generated by a single cross bridge is described on the basis of the experimental study of de Tombe and ter Keurs (14).

FLR. The most important advantage of the present model is its ability to describe the FLR and the FVR as functions of the activation level. The model reproduces the steepness of the FLR reported by Allen and Kentish (1) and explains the increase in calcium sensitivity with increasing sarcomere length. The model links the increased affinity of troponin with the increase of sarcomere length by the positive-feedback mechanism of the cooperativity; an increase in the sarcomere length increases the activation level. An increase in the activation level increases the number of cross bridges in the strong conformation and, through the cooperativity mecha-

nism, elevates calcium affinity, which further elevates the generated force. Thus the FLR in the cardiac muscle depends on the level of activation; interventions that increase the activation level, e.g., an increase in the free calcium (Fig. 5) or an increase in calcium affinity (Fig. 6), shift the FLR curve to the left and affect its steepness.

FVR—the shortening velocity. The major result of this study is that the dynamic loose-coupling model can describe a wide range of physiological phenomena in the intact muscle that were until now only experimentally determined. Of particular interest are the effects of the sarcomere length, free calcium transient, and activation level on the FVR, the unloaded velocity ($F = 0$), and the shortening deactivation.

As shown by *Eqs. 27 and 32*, the velocity of sarcomere shortening and the unloaded velocity depend mainly on three physiological parameters: the activation level, as defined by A_s , the rate of cross-bridge cycling from the weak to the strong conformation, as denoted by f , and the internal load stiffness, K_{PE} . Some brief comments on the properties of these parameters may help elucidate the physiological phenomena.

As discussed above, the activation level, and thus the shortening velocity, depends on the free calcium concentration, the sarcomere length, the time during contraction, and the affinity of troponin for calcium, which is determined by the cooperativity mechanism. As illustrated in Figs. 5 and 6, the free calcium transient, the sarcomere length, and the cooperativity determine the FLR, the ability of the muscle to generate force, and thus the activation level. The dependence of the shortening velocity on the free calcium and the sarcomere length was demonstrated by Daniels et al. (13) and Edman (15). Moreover they showed that the unloaded shortening velocity increases with the time during the twitch and reaches its maximum well ahead of the time of peak isometric contraction. This phenomenon is consistent with the present model, because the shortening velocity depends on state A_s , the activation level, which reaches its maximal level before the peak force (states T_s and U_s in Fig. 2). The present model demonstrates the combined effect of the free calcium and the sarcomere length on the activation level and thus on the shortening velocity.

The shortening velocity also depends on the rate of cross-bridge cycling from the weak to the strong conformation (f in *Eqs. 27 and 32*), as was postulated by Brenner and Eisenberg (10). This relation can explain the dependence of the shortening velocity and the unloaded velocity on the temperature (15), because the elevation of the temperature increases the rate of actomyosin ATPase activity (10).

Finally, the shortening velocity is inversely related to the internal load stiffness. The internal load in the cardiac muscle has a significant influence on the FVR, as postulated by Ford (17) and seen in *Eq. 27*. The different curves in Fig. 9 for different initial sarcomere lengths in the cardiac muscle cannot, unlike the skeletal muscle, be reduced and normalized to one characteristic curve (17). The internal load is especially significant at low levels of

activation and short sarcomere lengths (17), when the magnitude of the internal load is of the order of the developed force.

All the above physiological parameters affect the shortening velocity, and their influence is expressed in the theoretically developed Hill's equation. Note again that Hill's equation is obtained here by accounting for the mechanical feedback, whereby the velocity of filament shortening weakens cross-bridge conformation.

Unloaded shortening velocity. The unloaded velocity is derived from the FVR described by *Eq. 27* and thus depends on the free calcium level, sarcomere length, time during contraction, cooperativity, cross-bridge cycling rate, temperature, and internal load. As expressed in *Eq. 32* for high levels of activation, the unloaded shortening velocity reaches a plateau. Thus, in accordance with the findings of Edman (15), the maximal shortening velocity is constant at sarcomere lengths of 1.65–2.7 μm for high activation levels. Beyond this range, the internal load resistance to shortening at sarcomere lengths $< 1.65 \mu\text{m}$ and the parallel elastic stiffness at sarcomere length $> 2.7 \mu\text{m}$ is on the order of the activation level and affects the shortening velocity. Moreover, *Eq. 34*, which is obtained from *Eq. 32* and describes the dependence of the unloaded velocity on the peak isometric force, is identical to the experimentally derived expression obtained by de Tombe and ter Keurs (14).

The simulation of the FVR (Fig. 9), based on isometric-isotonic changeover experiments of Braunwald (7), demonstrates the importance of the instant during the twitch when the velocity is measured. Because the transition from the isometric to the isotonic regimen occurs earlier in the contraction as the isotonic load is reduced (Fig. 8), the activation level is also reduced. Thus, at low load levels, the activation level is low and the maximal unloading shortening velocity in this type of experiment is therefore lower than $V_{u,max}$. This conclusion strengthens the stipulated (13) importance of measuring the FVR at the same activation level or at the same instant during the contraction.

The simulations thus demonstrate the ability of the model to calculate the velocity of shortening at any level of activation and under various mechanical constraints. It is important to note that the FVR is not a constitutive law of the cardiac muscle but is derived on the basis of a physiological description of the control of contraction.

Shortening deactivation. The effect of the shortening velocity on the instantaneous force is often denoted "shortening deactivation," but the underlying phenomena are not well differentiated in the literature. Here the reduction in the force due to the shortening is related to 1) reduction in the sarcomere length and thus in the number of cross bridges in the single-overlap region (this mechanism has only a minor negligible effect), 2) reduction in the average force generated by each cross bridge, as postulated by de Tombe and ter Keurs (14), 3) decrease in the number of cross bridges in the strong conformation, i.e., cross-bridge weakening, as postulated by Eisenberg and Hill (16), and 4) reduction in the amount of bound calcium (27) and thus in the activation

level (state A_s), i.e., reduction in the ability of the muscle to hydrolyze more ATP (12) and to generate force. Note that this reduction in the activation level is not solely due to reduction in the sarcomere length but also to the cooperativity mechanism, whereby the affinity of troponin for calcium depends on the number of cycling cross bridges.

The phenomenon of shortening deactivation (17, 27) is thus obtained by the combined effect of the two feedback loops: the shortening velocity weakens cross-bridge cycling through the mechanical feedback, which leads to a decrease in the affinity of troponin for calcium through the cooperativity feedback, which further decreases the generated force.

Consistent with the studies of Leach et al. (29) and Sagawa et al. (34), the model describes (Eq. 40) the phenomena of the shortening deactivation and the calculated force deficit. Consistent with the mechanical feedback mechanism, the force deficit depends on 1) the velocity of shortening, 2) the duration of shortening, and 3) the force level. The ability of the model to describe this phenomenon strengthens the stipulated importance of the mechanical feedback and especially its dependence on the force level. It is noteworthy that Sagawa et al. took a similar approach to that of Leach et al. and measured the instantaneous difference between the ejecting and isovolumetric pressures in the isolated left ventricle. They demonstrated that the instantaneous ejection rate is the dominant cause for this pressure difference in the left ventricle. The correspondence between the present theoretical analysis and model simulations and these studies (29, 34) suggests that the model can be extended to describe the performance of the left ventricle in accordance with the studies of Sagawa and co-workers.

Advantages and limitations. The model allows a comprehensive quantitative description of the cardiac cycle and the intracellular control of contraction. The main advantage of the present model lies in its ability to describe the basic mechanical properties of the cardiac muscle: the FLR and the FVR as a function of the activation level and mechanical constraints. Moreover the model provides a "theoretical" physiological basis to Hill's equation for the FVR, as well as for the phenomenon of unloaded velocity and shortening deactivation on the basis of calcium kinetics and cross-bridge cycling.

The model also simulates the effect of the mechanical constraints, as load levels, on the free calcium transients. However, the model does not describe the control of calcium release from the sarcolemma and the SR but makes use of a simple phenomenological model (30) to describe these calcium currents. A more sophisticated model may eventually provide better insight, but the present model yields quite satisfactory results.

Conclusions. The proposed dynamic model has some special features that strengthen its credibility: 1) the model is based on calcium kinetics and on a biochemical model of cross-bridge cycling and does not depend on stationary measurements; 2) the activation function is well defined; 3) the model allows simulation of the

known mechanical phenomena of the cardiac muscle relating to one beat; 4) the model is capable of simulating the changes in the free calcium associated with different mechanical regimens; and 5) the model, given as a set of ordinary differential equations, can be used to study any mechanical and geometrical constraint.

The model is based on experimentally established biochemical processes and substantiates a number of important physiological stipulations. 1) Calcium binding to the low-affinity sites on the troponin is necessary for triggering cross-bridge turnover from weak to strong conformations; 2) calcium dissociation from low-affinity sites can occur before cross-bridge turnover to the weak conformation, hence the term loose-coupling model; 3) the number of the cross bridges in the strong conformation affects the affinity of troponin for calcium; this is the basis for the dominant cooperativity mechanism; 4) the cross-bridge turnover to the weak conformation is independent of the existence of bound calcium on the troponin; and 5) the velocity of filament sliding affects the turnover rate of the cross bridges from the strong to the weak conformation. Obviously, the success of the model strongly strengthens the validity of these stipulations.

It is hoped that the proposed model can be used in the construction of a comprehensive model of excitation-contraction coupling and energy consumption. Because the parameters of the model describe physiological rate reactions, there is reason to believe that the proposed model can be useful in evaluating the effect of various pathological processes that may affect calcium kinetics and cross-bridge cycling.

We thank Jack Tarshis for personal support and encouragement and Prof. Henk ter Keurs for some illuminating discussions.

This study was sponsored by the Women's Division, American Technion Society (New York) and supported in part by the Fund for the Promotion of Research at the Technion (to S. Sideman), the Henri Gutwirth Fund for the Promotion of Research (to S. Sideman), the Miriam and Aaron Gutwirth Memorial Fellowship (to A. Landesberg), and the Al and Phyllis Newman Endowment Fund.

Address for reprint requests: S. Sideman, Julius Silver Institute, Dept. of Biomedical Engineering, Technion-IIT, Haifa 32000, Israel.

Received 24 March 1993; accepted in final form 18 March 1994.

REFERENCES

1. Allen, D. G., and J. C. Kentish. The cellular basis of the length-tension regulation in cardiac muscle. *J. Mol. Cell. Biol.* 17: 821-840, 1985.
2. Allen, D. G., and J. C. Kentish. Calcium concentration in the myoplasm of skinned ferret ventricular muscle, following changes in muscle length. *J. Physiol. Lond.* 407: 489-503, 1988.
3. Allen, D. G., and S. Kurihara. The effect of muscle length on intracellular calcium transient in mammalian cardiac muscle. *J. Physiol. Lond.* 327: 79-94, 1981.
4. Allen, D. G., and G. L. Smith. The first calcium transient following shortening in isolated ferret ventricular muscle (Abstract). *J. Physiol. Lond.* 366: 83P, 1985.
5. Beyar, R., and S. Sideman. A computer study of the left ventricular performance based on fiber structure, sarcomere dynamics, and transmural electrical propagation velocity. *Circ. Res.* 55: 358-375, 1984.
6. Brandt, P. W., M. S. Diamond, J. S. Rulehik, and F. H. Schachat. Cooperative interactions between troponin-tropomyosin units extend the length of the thin filament in skeletal muscle. *J. Mol. Biol.* 195: 885-896, 1987.

7. **Braunwald, E.** *Heart Disease, A Textbook of Cardiovascular Medicine* (3rd ed.). Philadelphia, PA: Saunders, 1988, p. 394–401.
8. **Brenner, B.** Rapid dissociation and reassociation of actomyosin crossbridge during force generation: a newly observed facet of crossbridges action in muscle. *Proc. Natl. Acad. Sci. USA* 88: 10490–10494, 1991.
9. **Brenner, B.** Effect of Ca²⁺ on crossbridge turnover kinetics in skinned single rabbit psoas fibers: implication for regulation of muscle contraction. *Proc. Natl. Acad. Sci. USA* 85: 3265–3269, 1988.
10. **Brenner, B., and E. Eisenberg.** Rate of force generation in muscle: correlation with actomyosin ATPase activity in solution. *Proc. Natl. Acad. Sci. USA* 83: 3542–3546, 1986.
11. **Brutsaert, D. L., F. E. Rademakers, and S. U. Sys.** Triple control of relaxation: implications in cardiac disease. *Circulation* 69: 190–196, 1984.
12. **Chalovich, J. M., and E. Eisenberg.** The effect of troponin-tropomyosin on the binding of heavy meromyosin to actin in the presence of ATP. *J. Biol. Chem.* 261: 5088–5093, 1986.
13. **Daniels, M., M. I. M. Noble, H. E. D. J. ter Keurs, and B. Wohlfart.** Velocity of sarcomere shortening in rat cardiac muscle: relationship to force, sarcomere length, calcium and time. *J. Physiol. Lond.* 355: 367–381, 1984.
14. **De Tombe, P. P., and H. E. D. J. ter Keurs.** An internal viscous element limits unloaded velocity of sarcomere shortening in rat myocardium. *J. Physiol. Lond.* 454: 619–642, 1992.
15. **Edman, K. A. P.** The velocity of unloaded shortening and its relation to sarcomere length and isometric force in vertebrate muscle fibers. *J. Physiol. Lond.* 291: 143–159, 1979.
16. **Eisenberg, E., and T. L. Hill.** Muscle contraction and free energy transduction in biological system. *Science Wash. DC* 227: 999–1006, 1985.
17. **Ford, E. L.** Mechanical manifestations of activation in cardiac muscle. *Circ. Res.* 68: 621–637, 1991.
18. **Grabarek, Z., J. Grabarek, P. J. Leavis, and J. Gergely.** Cooperative binding to Ca²⁺-specific sites of troponin C in regulated actin and actomyosin. *J. Biol. Chem.* 258: 14098–14102, 1983.
19. **Greene, L. E., and E. Eisenberg.** Relationship between regulated actomyosin ATPase activity and cooperative binding of myosin to regulated actin. *Cell Biophys.* 12: 59–71, 1988.
20. **Guth, K., and J. D. Potter.** Effect of rigor and cycling cross-bridges on the structure of troponin-C and on the Ca²⁺ affinity of the Ca²⁺-specific regulatory sites in skinned rabbit psoas fibers. *J. Biol. Chem.* 262: 15883–15890, 1987.
21. **Hibberd, M. G., and B. R. Jewell.** Calcium and length-dependent force production in rat ventricular muscle. *J. Physiol. Lond.* 329: 527–540, 1982.
22. **Hill, A. V.** Heat of shortening and the dynamic constants of muscle. *Proc. R. Soc. Lond. B Biol. Sci.* 126: 136–195, 1938.
23. **Hofmann, P. A., and F. Fuchs.** Effect of length and crossbridge attachment on Ca²⁺ binding to cardiac troponin-C. *Am. J. Physiol.* 253 (*Cell Physiol.* 22): C90–C96, 1987.
24. **Hofmann, P. A., and F. Fuchs.** Evidence for force-dependent component of calcium binding to cardiac troponin-C. *Am. J. Physiol.* 253 (*Cell Physiol.* 22): C541–C546, 1987.
25. **Izakov, V. Y., L. B. Katsnelson, F. A. Blyakhman, V. S. Markhasin, and T. F. Shklyar.** Cooperative effects due to calcium binding by troponin and their consequences for contraction and relaxation of cardiac muscle under various conditions of mechanical loading. *Circ. Res.* 69: 1171–1184, 1991.
26. **Kentish, J. C., H. E. D. J. ter Keurs, L. Riccardi, J. J. J. Buxx, and M. I. M. Noble.** Comparison between the sarcomere length-force relations of intact and skinned trabeculae from rat right ventricle. *Circ. Res.* 58: 755–768, 1986.
27. **Lab, M. J., D. G. Allen, and C. H. Orchard.** The effect of shortening on myoplasmic calcium concentration and on action potential in mammalian ventricular muscle. *Circ. Res.* 55: 825–829, 1984.
28. **Landesberg, A., and S. Sideman.** Coupling calcium binding to troponin-C and crossbridge cycling kinetics in skinned cardiac cells. *Am. J. Physiol.* 266 (*Heart Circ. Physiol.* 35): H1260–H1271, 1994.
29. **Leach, J. K., A. J. Brady, B. J. Skipper, and D. L. Millis.** Effect of active shortening on tension development of rabbit papillary muscle. *Am. J. Physiol.* 238 (*Heart Circ. Physiol.* 7): H8–H13, 1980.
30. **Lee, J. A., and D. G. Allen.** EMD 53998 sensitizes the contractile proteins to calcium in intact ferret ventricular muscle. *Circ. Res.* 69: 927–936, 1991.
31. **Lombardi, V., G. Puazzesi, and M. Linari.** Rapid regeneration of actin-myosin power stroke in contracting muscle. *Nature Lond.* 355: 638–641, 1992.
32. **Peterson, J. N., W. C. Hunter, and M. R. Berman.** Estimated time course of calcium bound to troponin-C during relaxation in isolated cardiac muscle. *Am. J. Physiol.* 260 (*Heart Circ. Physiol.* 29): H1013–H1024, 1991.
33. **Robertson, S. P., P. Johnson, and J. D. Potter.** The time course of calcium exchange with calmodulin, troponin, paralbumin and myosin in response to transient increase in calcium. *Biophys. J.* 34: 559–569, 1981.
34. **Sagawa, K., L. Maughan, H. Suga, and K. Sunagawa.** *Cardiac Contraction and the Pressure-Volume Relationship.* Oxford, UK: Oxford Univ. Press, 1988, p. 86–88.
35. **Sperelakis, N.** *Physiology, and Pathophysiology of the Heart* (2nd ed.). New York: Kluwer, 1989, p. 1–15.
36. **Stephenson, D. G., A. W. Stewart, and G. J. Wilson.** Dissociation of force from myofibrillar MgATPase and stiffness at short sarcomere length in rat and toad skeletal muscle. *J. Physiol. Lond.* 410: 351–366, 1989.
37. **Sys, S., and D. L. Brutsaert.** Determinants of force decline during relaxation in isolated cardiac muscle. *Am. J. Physiol.* 257 (*Heart Circ. Physiol.* 26): H1490–H1497, 1989.
38. **Williams, D. L., L. E. Greene, and E. Eisenberg.** Cooperative turning on of myosin subfragment-1 ATPase activity by the troponin-tropomyosin-actin complex. *Biochemistry* 27: 6987–6993, 1988.
39. **Wong, A. L. K.** Mechanics of cardiac muscle, based on Huxley's model: mathematical simulation of isometric contraction. *J. Biomech.* 4: 529–540, 1971.
40. **Yue, D. T., E. Marban, and G. Wir.** Relationship between force and intracellular calcium in tetanized mammalian heart muscle. *J. Gen. Physiol.* 87: 223–424, 1986.
41. **Zahalak, I. G., and M. A. Shi-ping.** Muscle activation and contraction: constitutive relations based directly on crossbridge kinetics. *J. Biomech. Eng.* 112: 52–62, 1990.